

SLOSHING WAVES AND RESONANT MODES OF SLOSHING FLUID IN A 3D TANK

Bang-Fuh Chen

Professor, Department of Marine Environment and Engineering, National Sun Yat-sen University, Kaohsiung, Taiwan 804, e-mail: chenbf@mail.nsysu.edu.tw

Chih-Hua Wu

PH.D. student, e-mail: hua.keni@gmail.com

ABSTRACT

A developed time-independent finite difference method is used to solve for the sloshing waves in a three-dimensional tank with square basin. The 3D equations of motion of fluid are derived in moving coordinate system and complete six degrees of freedom of motion are included (surge/sway/heave/pitch/roll/yaw). Just for the demonstrate purpose, only the coupling effect of surge and sway motions are considered in the paper. The numerical scheme is validated by proper benchmark studies. Five types of sloshing waves were generated when the tank is excited by various excitation frequencies. The spectral analyses were made to identify the resonant frequencies of each type of wave. The clear evidence shows the solid correlation between the occurrence of the sloshing wave types and specific resonant modes.

1. INTRODUCTION

Free surface sloshing in a moving container is associated with various engineering problems, such as tankers on highways, liquid oscillations in large storage tanks caused by earthquakes, sloshing of liquid cargo in ocean-going vessels, and the motion of liquid fuel in aircraft and spacecraft. It is known that partially filled tanks are prone to violent sloshing under certain conditions, especially when near resonant excitation occurs. The large amplitude movement of the liquid can create high impact pressures on the tank walls, which in turn can cause structural damage and may even create moments that affect the stability of the vehicle which carries the container.

In the mid of 1970, Abramson (1966) provides a rather comprehensive review and discussion of analytic and experimental studies of liquid sloshing which apply in aerospace industry. The potential formulation of the problem is often used in studying sloshing such as Waterhouse (1994) and Ockendon et al. (1996) among many others. Most recently Faltinsen et al. (2003, 2005 and 2006) extended their asymptotic modal system to model nonlinear

sloshing in a 3D rectangular tank.

Besides the potential flow approaches, many numerical studies (computational fluid dynamics, CFD, simulation) of the problems with primitive variables were made, particularly for the fully nonlinear effects of the sloshing waves on free surface. The reported techniques handling wavy free surface include VOF, SOLA, SURF and also the σ -transformation technique to stretch the grid from the bed to surface. Most recently, Chen and Nokes (2005) developed a time-independent finite difference method to study viscous fluid sloshing in 2D rectangular tanks, the time varied moving boundary was mapped onto a time-independent domain through proper transformation functions and the coupled surge-pitch-heave motions are included.

Most reported studies were the tanks excited by limited exciting directions and with a fixed excitation frequency throughout the excitation. In reality, as the tank is excited by earthquake or assaulting waves, the excited directions are actually multi-degree of freedoms and the excitation frequency varies with time. In the three-dimensional model, the developed time-independent finite difference method (Chen and Nokes 2005) is extended to incorporate the incompressible and inviscid Navier-Stokes equations, fully nonlinear kinematic and dynamic free surface conditions in the analysis of the seismic response of sloshing fluid in a rectangular tank with a square basin. The main study of this paper simulates a 3-D tank undergoing only surge-sway motions with varying excited directions and only the transient phenomenon is recorded and studied. The tank excited in horizontal ground motion (coupled surge-sway motion) with various excitation angle θ (θ indicates the direction of horizontal ground motion) resulted in five kinds of sloshing waves (single-directional, diagonal, square-like, swirling and irregular waves) and the FFT (Fast Fourier Transform) spectral analysis was used to identify the dominant frequencies of each type of waves. The results show that the correlation between the occurrence of the sloshing wave types

and specific resonant modes is inseparable.

2. Mathematical Formulation

A fully non-linear model of inviscid 3-D waves in a numerical wave tank was developed. As shown in Fig 1, a rigid tank with breadth L , width B and still water depth d_0 . As the coordinate system is chosen to move with the tank motions (including surge, sway, heave, yaw, roll and pitch motions, see Fig. 1), the momentum equations can be derived and written as

$$\frac{\partial u}{\partial t} + u \frac{\partial u}{\partial x} + v \frac{\partial u}{\partial y} + w \frac{\partial u}{\partial z} = -g \sin \gamma - \frac{1}{\rho} \frac{\partial p}{\partial x} - \ddot{X}_c - (\ddot{\beta}z - \dot{\gamma}y) - (2\dot{\alpha}\dot{\beta} - \dot{\beta}^2 - \dot{\gamma}^2)x - 2 \times (\dot{\beta}w - \dot{\gamma}v) \quad (1)$$

$$\frac{\partial v}{\partial t} + u \frac{\partial v}{\partial x} + v \frac{\partial v}{\partial y} + w \frac{\partial v}{\partial z} = -g \cos \beta - \frac{1}{\rho} \frac{\partial p}{\partial y} - \ddot{Y}_c - (\dot{\gamma}x - \dot{\alpha}z) - (2\dot{\beta}\dot{\gamma} - \dot{\alpha}^2 - \dot{\gamma}^2)y - 2 \times (\dot{\gamma}u - \dot{\alpha}w) \quad (2)$$

$$\frac{\partial w}{\partial t} + u \frac{\partial w}{\partial x} + v \frac{\partial w}{\partial y} + w \frac{\partial w}{\partial z} = -g \sin \alpha - \frac{1}{\rho} \frac{\partial p}{\partial z} - \ddot{Z}_c - (\dot{\alpha}y - \dot{\beta}x) - (2\dot{\alpha}\dot{\gamma} - \dot{\alpha}^2 - \dot{\beta}^2)z - 2 \times (\dot{\alpha}v - \dot{\beta}u) \quad (3)$$

where u , v and w are velocity components in x , y and z directions, \ddot{x}_c , \ddot{y}_c and \ddot{z}_c are the acceleration components of tank in x , y and z directions; $(\dot{\alpha}$, $\dot{\beta}$, $\dot{\gamma})$ and $(\ddot{\alpha}$, $\ddot{\beta}$, $\ddot{\gamma})$ are the corresponding angular velocities and accelerations with respect to x , y and z -axes, p is the pressure, ρ is the fluid density and g the acceleration of gravity. Taking partial differentiation of Eqs. (1), (2) and (3) with respect to x , y and z respectively, and summing the results, one can obtain the following pressure wave equation which is made to solve for the pressure.

$$\begin{aligned} \frac{\partial^2 p}{\partial x^2} + \frac{\partial^2 p}{\partial y^2} + \frac{\partial^2 p}{\partial z^2} = & -\rho \frac{\partial}{\partial x} \left(u \frac{\partial u}{\partial x} + v \frac{\partial u}{\partial y} + w \frac{\partial u}{\partial z} \right) \\ & -\rho \frac{\partial}{\partial y} \left(u \frac{\partial v}{\partial x} + v \frac{\partial v}{\partial y} + w \frac{\partial v}{\partial z} \right) -\rho \frac{\partial}{\partial z} \left(u \frac{\partial w}{\partial x} + v \frac{\partial w}{\partial y} + w \frac{\partial w}{\partial z} \right) \\ & -2\rho[\dot{\alpha}\dot{\beta} + \dot{\beta}\dot{\gamma} + \dot{\alpha}\dot{\gamma}] - (\dot{\alpha}^2 + \dot{\beta}^2 + \dot{\gamma}^2) - 2\rho[\dot{\alpha}(\frac{\partial v}{\partial z} - \frac{\partial w}{\partial y}) \\ & + \dot{\beta}(\frac{\partial w}{\partial x} - \frac{\partial u}{\partial z}) + \dot{\gamma}(\frac{\partial u}{\partial y} - \frac{\partial v}{\partial x})] \end{aligned} \quad (4)$$

The continuity equation for incompressible flow is

$$\frac{\partial u}{\partial x} + \frac{\partial v}{\partial y} + \frac{\partial w}{\partial z} = 0 \quad (5)$$

The kinematic free surface boundary condition is

$$\frac{\partial h}{\partial t} + u \frac{\partial h}{\partial x} + v \frac{\partial h}{\partial y} + w \frac{\partial h}{\partial z} = v \quad (6)$$

and the dynamic free surface condition is $p = 0$ and the boundary condition at the solid walls must satisfied momentum equations. Instead of using boundary fitted coordinate (BFC) system, we used simple mapping functions to remove the time-varied boundary of the fluid domain. The irregular tank walls and tank bottom can be mapped onto a cubic one by the proper coordinate transformations as

$$x^* = \frac{x - b_1(y, z)}{b_2(y, z) - b_1(y, z)}, y^* = 1 - \frac{y + d(x, z)}{h(x, z, t)}, z^* = \frac{z - b_3(x, y)}{b_4(x, y) - b_3(x, y)} \quad (7)$$

where the instantaneous water surface, $h(x, z, t)$, is a single-valued function measured from tank bottom, $d(x, z)$ represents the vertical distance between still water surface and tank bottom, b_1 and b_2 are horizontal distance from the x -axis to the west and east walls respectively, and b_3 and b_4 are horizontal distance from the z -axis to the north and south walls respectively, (see Fig.1). The coordinates (x^*, z^*) can be further transformed so that the layer near the free surface, tank bottom and tank wall will be stretched by

$$\begin{aligned} X &= \lambda_1 + (x^* - \lambda_1) e^{\kappa_1 x^* (x^*-1)} \\ Y &= \lambda_2 + (y^* - \lambda_2) e^{\kappa_2 y^* (y^*-1)} \\ Z &= \lambda_3 + (z^* - \lambda_3) e^{\kappa_3 z^* (z^*-1)} \end{aligned} \quad (8)$$

The constants κ_2 and λ_2 control the mesh sizes near free surface and tank bottom. Similarly, the constants $\kappa_{1,3}$ and $\lambda_{1,3}$ map irregular finite difference mesh sizes near tank wall to the regular ones in the computational domain (X, Y, Z) . Thus, the geometry of the flow field and the meshes in the computational domain $(X-Y-Z$ system) become time-independent throughout the computational analysis.

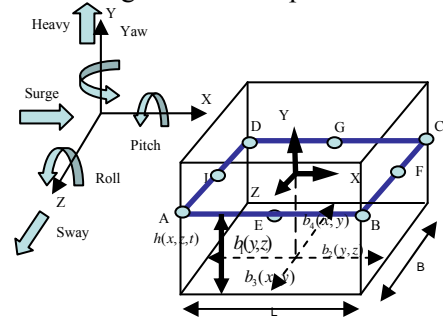


Figure 1: Definition Sketch.

3. Finite Difference Method

The numerical method used in this study is based on a finite difference method. There are many finite difference and volume method for evaluating free

surface. The most famous schemes are SURF, MAC and VOF methods and those methods need complicate computer programming in treating the time varied free surface boundary and updating computational meshes. Alternately, in the present study, the time-varied free surface boundary is transformed to a time-independent free surface in the $x^*-y^*-z^*$ domain and no boundary tracing is needed during the calculation. A single value height function is assumed and is evaluated by solving the kinematic free surface condition. In a three-dimensional analysis, the fluid flow is solved in a cubic mesh network of the transformed domain. The staggered grid system is used in the analysis (see Fig 2). The Crank-Nicholson iteration scheme and Gauss-Seidel Point successive over-relaxation iteration procedures are used to calculate velocity and pressure, respectively. The detailed iteration procedure is similar that reported in Chen and Roger (2005) and is omitted in the manuscript.

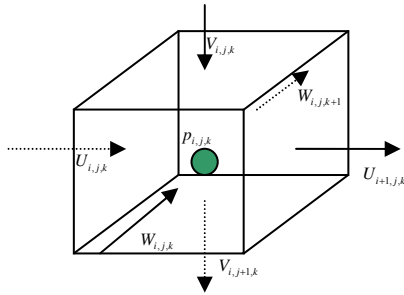


Figure 2: The staggered grid system.

4. Result and Discussion

In the present study, a rectangular tank with ratio breadth / width = $L / B = 1$, still water depth / breadth = $d_0 / L = 0.25$ are used in most of the simulations. Although the surge, sway, heave, pitch, roll, and yaw motions are considered in this study, the main focus of this paper is a tank under coupled surge-sway motion. The ground acceleration of surge, and sway motion are given as, and respectively, where, X_0 and Z_0 are the maximum excited amplitudes; and ω_x and ω_z are the corresponding excited frequency with respect to surge and sway motion.

4.1 Verification

In order to validate the accuracy of numerical simulation, the results obtained from the present numerical model are compared with those reported in the literature for the benchmark tests. The present results for the tank under surge motion agree greatly with Faltinsen's (2005) theoretical and experimental results as shown in Fig.3. The results for diagonal excitation produced by Kim (2001) also show great

agreement with the present study as shown in Fig.4. Thus, the present numerical model can be verified by the benchmark tests mentioned above.

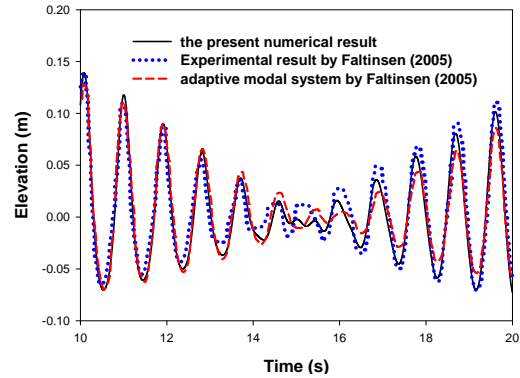


Figure 3: The wave history on tank's walls under surge motion, the ratio d_0 / L and $d_0 / B = 0.5$. Tank's displacement $a_0 / L = 0.0078$, $\omega_x = 1.037\omega_1$, ω_1 : the first natural frequency of the tank.

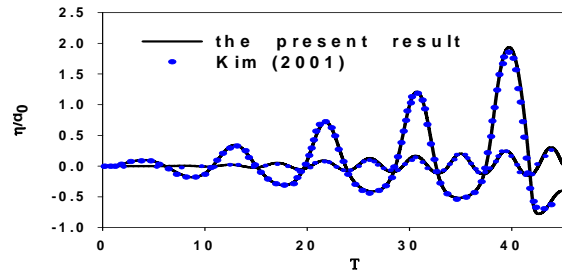


Figure 4: The wave history on tank's corner under Surge- Sway (diagonal) motion, the ratio d_0 / L and $d_0 / B = 0.25$, tank's displacement $a_0 / L = 0.0093$, $\omega_x = \omega_z = 0.99\omega_1$.

4.2 Sloshing waves in tanks

Five types of sloshing waves are introduced simply in this section. The single-directional waves which means waves slosh in the direction as well as the tank motion. The phenomenon of square-like waves corresponds to waves traveling primarily on two opposite sides of the tank. The diagonal wave sloshing in the tank was firstly investigated by Miles (1994), and the wave is basically sloshing in diagonal direction of the tank. As the waves slosh irregularly inside the tank, are termed irregular or chaotic waves. When waves move along the tank walls in a clockwise or counterclockwise direction, they are referred to as "swirling" waves. The swirling waves only appear as the tank under resonant forcing.

4.3 Spectral analysis

In this section, the spectral analyses are made to obtain the dominant resonance frequencies of each

type of the sloshing waves mentioned section 4.2. It is well known that the resonant sloshing resulted from the first fundamental frequency is called primary resonance of the tank. If the tank is excited with a frequency away from the first fundamental mode of the tank, the secondary resonance also can be triggered due to the effects of the other natural modes of the tank system.

Fig. 5 presents the spectral analyses for each type of sloshing waves, and the plots in the box at the right-upper corner are the corresponding wave histories. For excited angles = 5° and 45° , the excitation frequency = $0.4 \omega_1$, the single direction and diagonal wave occurs respectively. Two resonant peaks are identified in their spectral analyses, one is corresponding to the first fundamental frequency and the other is to the excitation frequency and the latter is the dominant one. For excited angles = 5° , and excitation frequency increases to $1.5 \omega_1$, the square-like wave presents and the dominant resonant frequency is the first fundamental frequency and the other resonant frequency is also the excitation frequency. For the same excited angle but the excitation frequency nears the first fundamental frequency, the secondary resonance, in addition to the primary resonance, occurs and is corresponding to $\omega_{2,2}$. And this secondary resonance is likely related to the occurrence of the swirling waves since the spectral analyses of the other cases of swirling waves all present a resonant peak corresponding to $\omega_{2,2}$.

As the excitation frequency further increase to $2.3 \omega_1$, the irregular wave occurs. Although the dominant resonant frequency is the first fundamental mode, several secondary resonances present and they are corresponding to modes $\omega_{3,0}$ and $\omega_{5,0}$ and they are also likely related to the occurrence of irregular waves. The said phenomenon may be clarified by the aid of the nature of the mode shape of the resonant modes as stated in the next section.

4.4 Sloshing waves and resonant modes

The natural modes and modal system obtained by Faltisen et al. suggested that two subclasses of wave patterns exist. The first one consists of two-dimensional Stokes wave pattern, and the corresponding waves are called as planar waves (Miles, 1994),

$$\begin{aligned}\phi_m^{(1)}(x) &= \cos\left[m\pi\left(x + \frac{1}{2}\right)\right] \\ \phi_n^{(2)}(y) &= \cos\left[n\pi r\left(y + \frac{1}{2r}\right)\right]\end{aligned}\quad (9)$$

The second subclass is the three dimensional

wave pattern given by the multiple of two Stokes waves

$$\phi_m^{(1)}(x)\phi_n^{(2)}(y) \quad (10)$$

Faltisen also suggested the mixed modes and the combination of the two Stokes modes to represent three-dimensional wave patterns. As stated in the previous section, the major resonant frequency can be identified from the spectral analysis of each type of sloshing wave. For diagonal wave, two resonant peaks occur and they are corresponding to the first natural mode of the system and excitation frequency. The diagonal wave is generated by a tank under couple surge and sway motions with excited angle = 45° , and the mode of $\omega_{0,1}$ and $\omega_{1,0}$, therefore, might provide equal effect on sloshing wave. Fig.6 depicts the mode shape of combining $\omega_{0,1}$ and $\omega_{1,0}$, and the resulting mode shape apparently likes a diagonal wave sloshing in the tank. Again under a diagonal forcing with the excitation frequency = $1.5 \omega_1$, the sloshing wave pattern changes to square-like wave. Fig. 7 depicts the square like wave patterns and the resonant mode shape. The spectral analysis of a square like wave presents two peaks, and they are also corresponding to the first fundamental frequency and excitation frequency. The combination of mode of $\omega_{1,0}$ and $\omega_{0,1}$ with 0.5 weight is depicted in Fig. 7 and the terraced planes at the diagonal corners are seen in the figure. Fig. 7 demonstrates a clear evidence of the solid correlation between sloshing surface patterns and resonant modes.

As the excitation frequency nears the first fundamental mode, the sloshing wave becomes swirling and the spectral analysis indicates a occurrence of small resonant peak of $\omega_{2,2}$. The corresponding mode shape can be obtained from the multiple of Stokes modes of $\omega_{2,0}$ and $\omega_{0,2}$. Fig.8 shows the mode shape of $\omega_{2,2}$ and the subplots of the figure are the surface contour of the swirling wave patterns. The relative surface peak might occur at four corners of the tank, mid point of four walls and the center of the tank surface. The surface contour plots, once again, demonstrate the close relationship between resonant mode and the sloshing wave patterns.

The spectral analysis of irregular waves indicates the resonant peaks of $\omega_{1,0}$, $\omega_{3,0}$, and $\omega_{5,0}$, and the mode shape of the combination of three resonant modes and the corresponding surface wave contour of are depicted in Fig. 9. As shown in the figure, similar evidence of correlation between resonant modes and surface wave patterns also can be found in the case of irregular waves.

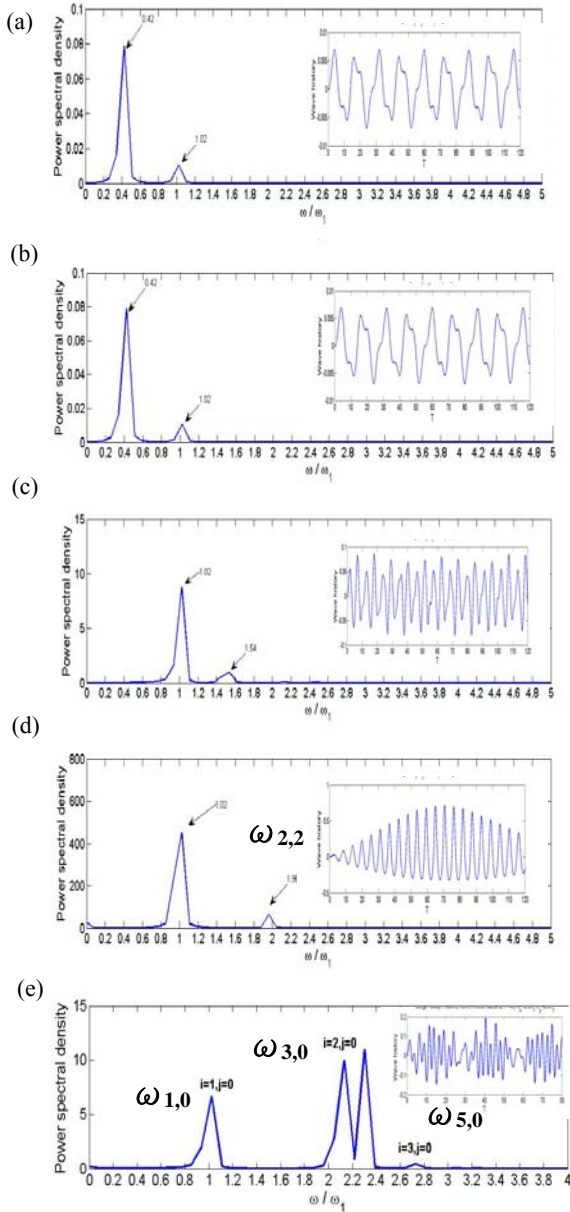


Figure 5: The spectral analysis of
 (a) Diagonal wave ($\theta = 45^\circ, \omega = 0.4\omega_1$),
 (b) Single direction wave ($\theta = 5^\circ, \omega = 0.4\omega_1$),
 (c) Square-like wave ($\theta = 5^\circ, \omega = 1.5\omega_1$),
 (d) Swirling wave and ($\theta = 5^\circ, \omega = 0.97\omega_1$)
 (e) Irregular wave ($\theta = 5^\circ, \omega = 2.3\omega_1$)

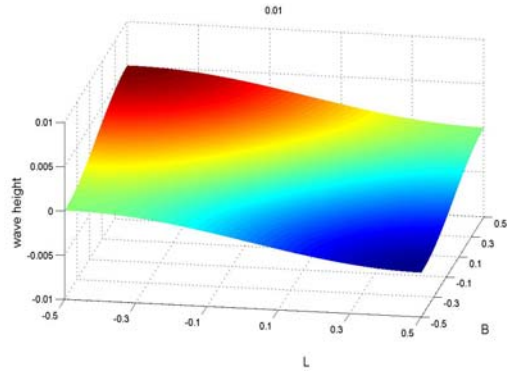


Figure 6: Diagonal wave patterns and resonance mode.

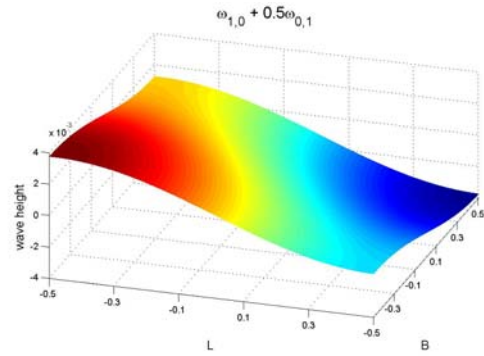
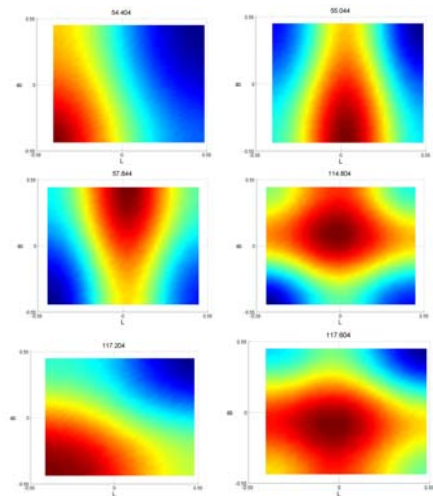
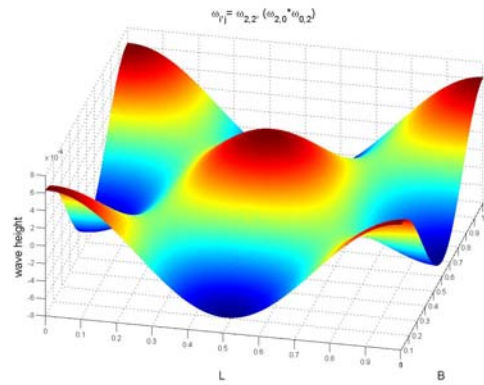


Figure 7: Square like waves patterns and resonance mode.



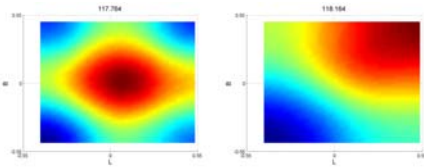


Figure 8: Swirling wave patterns and resonance mode.

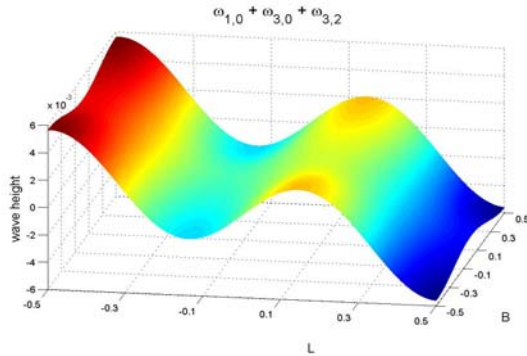


Figure 9: Irregular wave patterns and resonance mode

5. CONCLUSION

The developed time-independent finite difference method is extended to solve the incompressible and inviscid Navier-Stokes equations, fully nonlinear kinematic and dynamic free surface conditions in a rectangular tank with a square basin. The main study of this research simulates a 3-D tank undergoing different combination of motions with varying vibrating directions. The comparison of the results obtained by present simulation and those of reported data shows the acceptance and accuracy of the proposed numerical scheme. The following conclusions are reached:

1. Five types of sloshing waves are observed and they are quite related to the excitation frequency. As the sloshing frequency closes to the first fundamental mode, the swirling wave patterns occur. The other wave types, square-like and irregular wave patterns were also observed in the literatures when the tank is under near resonant excitation. In the present study, the square-like wave and irregular wave also can be triggered when the excitation frequency is far away from the first fundamental frequency with excited angle = 5° . Since the swirling wave is generated by the near resonant excitation, the swirling wave displacements at the corners are the largest among those of all types of sloshing waves.
2. The spectral analyses of five types of sloshing waves were made and the resonant peaks are corresponding to the primary mode and excitation frequency in the types of the diagonal,

single direction and square like waves. For swirling wave, a secondary resonance of mode $\omega_{2,2}$ occurs in addition to the primary resonance. For irregular waves, the resonant peaks of primary mode and excitation frequency do exist, however, the secondary resonances of odd modes $\omega_{3,0}$ and $\omega_{5,0}$ also present.

3. The shape of the resonant modes and the surface contour of the wave pattern demonstrate a clear evidence of the solid correlation between the occurrence of each type of the sloshing waves and corresponding resonant modes.

6. REFERENCES

- Abramson, H. N., 1966, The dynamics of liquids in moving containers. NASA Rep. SP 106.
- Chen, B.F., Nokes, R., 2005, Time-independent finite difference analysis of fully non-linear and viscous fluid sloshing in a rectangular tank. *J. Comput. Phys.*, **209**, 47-81.
- Faltinsen, O. M., Rognrbakke O. F., Timokha, A. N., 2003. Resonance three-dimensional nonlinear sloshing in a square-base basin. *J. Fluid Mech.*, **487**, 1-42.
- Faltinsen, O. M., Rognrbakke O. F., Timokha, A. N., 2005. Resonant three-dimensional nonlinear sloshing in a square-base basin. Part 2. Effect of higher modes. *J. Fluid Mech.*, **523**, 199-218.
- Faltinsen, O. M., Rognrbakke O. F., Timokha, A. N., 2006, Resonant three-dimensional nonlinear sloshing in a square-base basin. Part 3. Base ratio perturbations. *J. Fluid Mech.*, **551**, 93-116
- Kim, Y., 2001. Numerical simulation of sloshing flows with impact loads. *Appl. Ocean Res.*, **23**, 53 – 62.
- Miles, J. W., 1994, Faraday waves: rolls versus squares. *J. Fluid Mech.*, **269**, 353 – 371
- Ockendon, J. R., Ockendon, H., Waterhouse, D.D., 1996, Multi-mode resonances in fluids. *J. Fluid Mech.*, **315**, 317-344.
- Waterhouse, D. D., 1994, Resonant sloshing near a critical depth. *J. Fluid Mech.*, **281**, 313-318